University of Huddersfield Repository

Beverley, Katharine J, Clint, John H. and Fletcher, Paul D. I.

Evaporation rates of structured and non-structured liquid mixtures

Original Citation

This version is available at http://eprints.hud.ac.uk/id/eprint/16332/

http://eprints.hud.ac.uk/

PCCP

Evaporation rates of structured and non-structured liquid mixtures

Kate J. Beverley, John H. Clint and Paul D. I. Fletcher*

Surfactant Science Group, Department of Chemistry, University of Hull, Hull, UK HU6 7RX.
E-mail: P.D.Fletcher@chem.hull.ac.uk

We have used a gravimetric technique to measure the rate of evaporation of a volatile liquid in mixtures with a second, involatile component under conditions of controlled gas flow. A range of non-structured and structured mixtures were investigated in order to examine whether the rate limiting step for evaporation may switch from vapour diffusion across the stagnant gas layer above the liquid to mass transfer within the liquid mixture. Evaporation rates of pentane and hexane from mixtures with squalane (involatile) show excellent agreement with rates calculated on the basis that vapour diffusion across a stagnant gas layer is rate limiting and that mass transfer within the liquid mixture is fast. Hexane gelled by the addition of silica particles is found to evaporate at a rate very similar to that for un-gelled hexane because the equilibrium vapour pressure of hexane is unaffected by silica particle addition. Water evaporation rates from mixtures with the non-ionic surfactant n-dodecyl hexaoxyethylene glycol ether ($C_{12}E_6$) were found to be up to 10 times slower than calculated vapour space diffusion controlled rates owing to the slow development of concentration gradients within these highly structured liquid mixtures.

Evaporation rates are of interest from a number of viewpoints including assessment of hazards arising from the spillage of volatile liquids, drying processes, release of volatile active components such as perfumes from commercial products and the retardation and control of evaporation by adsorbed monolayers or entrapment of the liquid within colloidal microstructures such as porous solids. Following the development of a simple gravimetric technique to measure evaporation rates from liquids into a controlled gas flow,[1] we have previously investigated evaporation rates of pure liquids,[1] liquids contained within porous solids[2] and from micro-emulsions.[3] In general, evaporation can be rate-limited by one of three possible processes. Firstly, in the experimental geometry used here, vapour diffusion across the stagnant gas layer (thickness h) above the liquid may be rate-determining. Secondly, there may be a significant energy barrier to the process of evaporating molecules leaving or entering the liquid/vapour surface. Thirdly, evaporation of a volatile species from a multi-component liquid mixture may generate concentration gradients within the liquid and thus mass transfer within the liquid may be rate-determining. For the case of pure liquid evaporation, no concentration gradients are generated within the liquid and the rate is determined by either the first or second process. For a range of pure liquids in the experimental geometry used here, measured evaporation rates are accurately predicted on the basis of a model assuming that the rate of vapour diffusion across the stagnant gas layer is rate-limiting.[1]

In the present study we have investigated a range of mixtures including unstructured liquid alkane mixtures, alkanes gelled by addition of colloidal particles (structured) and mixtures of water and a non-ionic surfactant which, depending on composition, exhibit a variety of highly structured lyotropic mesophases. Intuitively, one would expect that a greater degree of microstructuring within the liquid would slow mass transfer within the liquid phase (by diffusion or convection) and hence induce a switch from vapour phase diffusion control to liquid phase mass transfer control.

Experimental

Water was purified by reverse osmosis and passed through a Milli-Q reagent water system. n-Pentane (Aldrich, 98%), n-hexane (Beecroft and Partners, 99%), 2,6,10,15,19,23-hexamethyltetracosane (squalane, Aldrich, 99%) were columned twice over alumina to remove polar impurities. The non-ionic surfactant n-dodecyl hexaoxyethylene glycol ether ($C_{12}E_6$) was a chromatographically pure sample provided by Nikkol (Japan) and was used as received. Silica particles (partially hydrophobic, type H30) used to produce gel mixtures with hexane were obtained from Wacker Chemie. All mixture samples were prepared by direct weighing into the sample tube used for evaporation rate measurements. Hexane gels were prepared by dispersion of the silica particles into the solvent using a high-intensity ultrasonic vibracell processor (Sonics and Materials, 3 mm tip diameter) operating at 20 kHz and up to 10 W for two minutes. Viscous samples were heated and mixed to ensure initial homogeneity and re-weighed prior to measurement to take account of any evaporation losses during preparation.

The apparatus for measurement of the evaporation rates is described fully in ref. 1. Briefly, the sample is contained in a cylindrical glass sample tube (inner diameter 17.89 mm) suspended from a Precisa 125A balance. Dry nitrogen gas is passed through a column of activated charcoal (Puritube supplied by Phase Sep.) to remove any impurities and a flow meter to record the gas volume flow rate. The purified nitrogen stream flows through a thermostatting coil and enters the measurement vessel through an annular opening of approximately 1 mm gap. The gas then flows vertically upwards around the sample tube and emerges from the top of the vessel. The vessel containing the suspended sample tube is contained within a stirred, thermostatted outer vessel. Sample mass loss (± 0.0001 g) is recorded on the Precisa balance and logged into an EXCEL spreadsheet using a PC equipped with TAL Technologies WinWedge software which allows data transfer from the RS232 interface of the balance. Evaporation

rates are then obtained by numerical differentiation of the measured mass loss curves. We have shown previously[1] that, for the evaporation rates encountered in this study, there is no significant cooling of the sample during the evaporation, *i.e.* the sample remains at the thermostatted temperature.

All measurements were made at 25.0 °C.

Results and discussion

We consider the rate of loss of vapour from a sample containing a mass m of liquid with a thickness h of stagnant gas phase above it. The value of h is equal to the height of the liquid surface and the mouth of the sample tube. As described fully in ref. 1, at high gas flow rate the evaporation rate E (equal to the liquid mass loss per unit time) reaches a gas flow rate independent limit given by:

$$E = -\frac{\mathrm{d}m}{\mathrm{d}t} \approx \frac{MADPz}{hRT} \qquad (1)$$

where M is the molecular weight of the evaporating species, A is the surface area of the sample, D is the diffusion coefficient of the evaporating species in the stagnant gas space, P is the equilibrium vapour pressure, R is the gas constant and T is the absolute temperature. The parameter z is a factor which allows for the counter current flow of the second gas component (nitrogen) within the stagnant layer and is given by:

$$z = \left[\frac{P_{\mathrm{atm}}}{p} \ln\left(\frac{1}{1 - (P/P_{\mathrm{atm}})} \right) \right] \qquad (2)$$

The factor z is significantly different from unity only when the vapour pressure P of the volatile species is of comparable magnitude to the atmospheric pressure P_{atm}. For this study, the flow rate of dry nitrogen was kept constant at 1920 ml min^{-1}, sufficiently high that eqn. (1) is valid. The same sized sample tube was used for all measurements and thus the area A was constant (251.4 mm^2). The initial value of h (the stagnant layer thickness) varied from run to run but was typically around 22 mm and the initial liquid depth was around 15 mm.

Liquid mixtures

We first consider liquid mixtures containing a volatile species (either pentane or hexane) and an involatile species (squalane). The equilibrium vapour pressure of the volatile component in the mixture is given by

$$P = \gamma P_{\mathrm{o}} X \qquad (3)$$

where P_{o} is the vapour pressure of the pure component, X is the mole fraction of the volatile species and γ is the activity coefficient. The activity scale used here corresponds to $\gamma = 1$ for $X = 1$ and the vapour–gas mixture is assumed to behave ideally. The variation of γ with X for squalane mixtures with a range of linear alkanes has been measured by Ashworth and Everett.[4] Using the equations and parameter values found by Ashworth and Everett to accurately fit their experimental data, the variation of γ with X for pentane and hexane mixtures with squalane was calculated as shown in Fig. 1.

For evaporating liquid mixtures, the composition becomes richer in the less volatile species as evaporation proceeds and hence P changes with time. Substitution of eqn. (3) into eqn. (1), calculation of X from the liquid mass remaining at time t and incorporation of the activity coefficient correction allows the accurate calculation of evaporation rate over the whole time course. Values of vapour diffusion coefficients, vapour pressures and liquid densities required for the rate calculations are summarised in Table 1. Fig. 2 compares measured evaporation rates for the pentane–squalane and hexane–squalane mixtures with calculations made in this way, from which it can be seen that the agreement is excellent. Fig. 2 provides clear evidence that no significant concentration gradients are
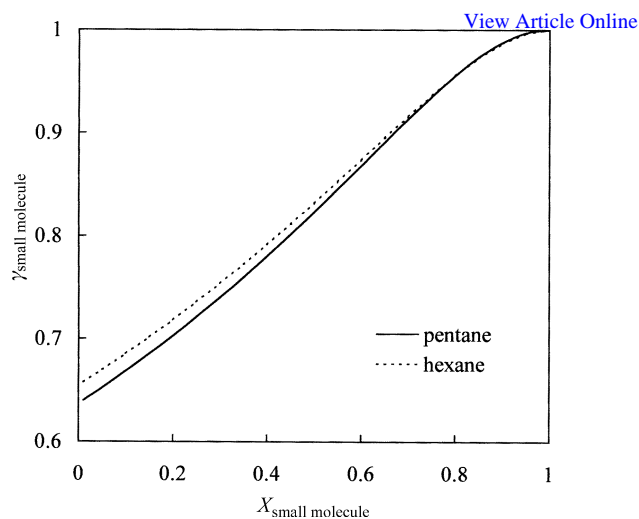

Fig. 1 Variation of activity coefficients with composition for pentane and hexane in mixtures with squalane at 25 °C. The lines are calculated as described in the text.

developed within the liquid mixtures as evaporation proceeds, *i.e.* the surface concentration of the evaporating species remains equal to the overall composition. As seen for pure liquids, there is no significant energy barrier hampering transport across the liquid/vapour surface. It is concluded that diffusion across the stagnant gas layer forms the rate-limiting process in these unstructured liquid mixtures.

It is highly likely that the uniformity of composition in the liquid phase is the result of convection induced by the evaporation at the liquid/vapour interface. Loss of pentane or
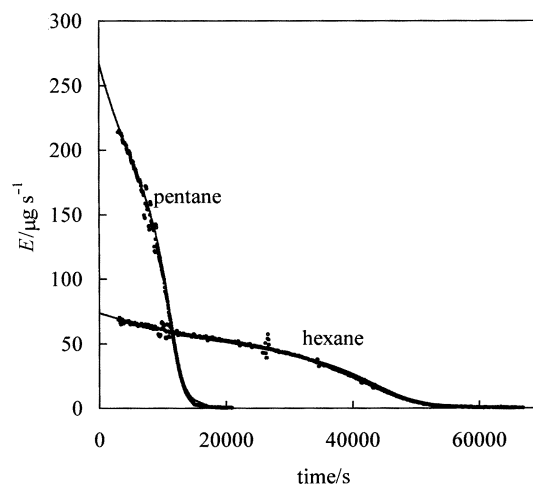

Fig. 2 Measured (solid circles) and calculated (solid lines) evaporation rates *vs.* time for mixtures of pentane and hexane with squalane. In each run, the mixtures initially contained approximately 0.4 g of squalane and 2.1 g of the volatile component.

Table 1 Values of vapour pressures P_{o}, diffusion coefficients D and densities ρ used in the calculation of evaporation rates at 25 °C. Values of D and P_{o} were taken from ref. 1 and references therein. Densities were taken from ref. 4 and 5

Component	P_{o}/Pa	$D/10^{-6}$ m^2 s^{-1}	ρ/kg m^{-3}
Pentane	68 368	8.42	621.2
Hexane	20 198	7.90	654.7
Water	3168	24.0	997.1
Squalane	—	—	804
$C_{12}E_6$	—	—	1000[a]

[a] Estimated value.

hexane from the mixtures with squalane will cause (a) a slight cooling of the surface region and (b) a local increase in the mole fraction of squalane at the surface. Both of these effects will produce an increase in density of the surface region compared with that in the bulk liquid. This produces a gravitational instability which sets up an array of small convective cells, the net result of which is good mixing of the liquid. Such effects have been observed during the evaporation of water from aqueous sucrose solutions where polygonal cells a few mm across are formed and liquid velocities of a few μm s^{-1} (measured using latex tracer particles) are established.[6]

Hexane gelled with solid particles

We next consider the evaporation of hexane gelled by the addition of silica particles. In this case, the silica particles (although intimately mixed with the hexane) form a separate and immiscible phase. Under these conditions the vapour pressure of the hexane remains constant and equal to P_o for all compositions. Fig. 3 shows the evaporation rate *vs.* time for a gel sample initially containing 2.2 g of hexane mixed with 0.26 g of silica particles. The initial gel was highly viscous and showed no flow when the sample tube was inverted. Visual observation of evaporating samples showed that partial evaporation from the gel produced a gel layer sitting below a very loosely packed powder layer of silica particles from which the hexane had been lost. The rate calculated assuming that vapour diffusion across the stagnant gas layer is rate limiting shows reasonable agreement with the measured values up to times of 30 000 s or so. As shown in Fig. 4, by this time the overall mass fraction of hexane has dropped to approximately 0.6. At higher times (corresponding to lower hexane mass fractions) the measured rates fall below the calculated values, probably as a result of two main effects. Firstly, the loosely packed silica powder layer on top of the gel layer may serve to slow the vapour diffusion rate slightly by an obstruction effect. Erratic partial collapse of this layer may be responsible for the less smooth appearance of the evaporation rate curves as compared with non-gelled samples (*e.g.* Fig. 2). Secondly, at very low hexane mass fractions towards the end of the evaporation, the small amount of hexane remaining is expected to form small liquid bridges at the points of contact between two adjacent particles. The liquid surfaces of these bridges are highly curved resulting in a lowering of the hexane vapour pressure according to the Kelvin equation. As noted previously for water contained within porous solids,[2] curvature induced vapour pressure lowering results in a reduced

Fig. 4 The data of Fig. 3 replotted as a function of mass fraction of hexane in the hexane–silica particle mixtures.

evaporation rate. Apart from these minor effects, hexane gelled using silica particles shows similar evaporation rate profiles to pure, non-gelled hexane with vapour diffusion across the stagnant gas layer being rate-limiting.

Water–surfactant mixtures

The third type of mixture investigated consisted of water (the volatile component) mixed with the non-ionic surfactant n-dodecylhexaoxyethylene glycol ether $C_{12}E_6$ (involatile). In these mixtures, the surfactant induces both a (composition dependent) lowering of the water vapour pressure according to eqn. (3) and a microstructuring of the liquid by the spontaneous self-assembly of the surfactant into a variety of ordered mesophases. Water activity coefficients as a function of water mole fraction (reproduced from ref. 7) are shown in Fig. 5. The solid curves show the polynomial functions fitted to the experimental data of ref. 7 which were used to describe the relation between γ and X. These relationships were combined with eqn. (1)–(3) in order to calculate the evaporation rate expected if gas diffusion across the stagnant gas layer is rate limiting.

It is relevant to note here that the presence of an adsorbed monolayer of $C_{12}E_6$ at the liquid/gas surface does not retard water evaporation significantly. Evaporation rate retardation has only been observed for condensed monolayers of long (typically 20 carbon atom) hydrocarbon chain, water insoluble
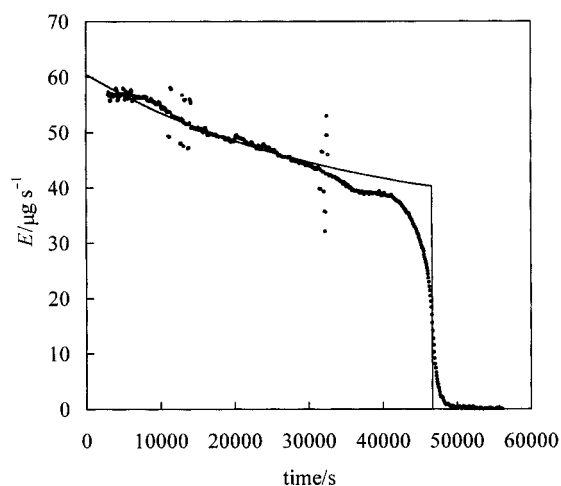

Fig. 3 Evaporation rate *vs.* time for hexane gelled with silica particles. The solid line shows the rate calculated on the basis that the hexane has a composition independent vapour pressure equal to that of pure hexane. The mixture initially contained 0.2607 g of silica and 2.1801 g of hexane.
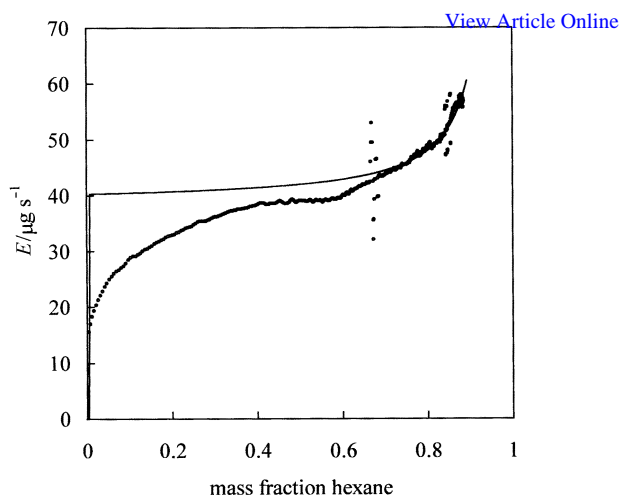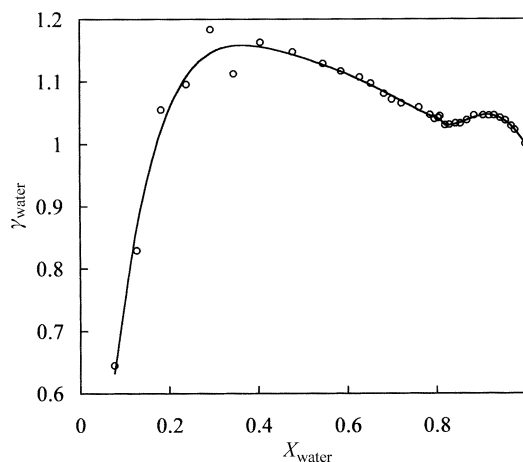

Fig. 5 Variation of γ_{water} with X_{water} for mixtures with $C_{12}E_6$. The solid lines show the polynomial functions used to fit the experimental data from ref. 7.

species at very high surface concentrations (typically >5 chains per nm^2).[8] Adsorbed monolayers of soluble surfactants such as $C_{12}E_6$, with maximum surface concentrations of around 2 chains per nm^2, are highly disordered and show no evaporation retardation.[9]

The phase boundaries for water/$C_{12}E_6$ are summarised in Table 2 (ref. 7 and 10). With increasing $C_{12}E_6$ concentration, the phase sequence is isotropic micellar dispersion (L_1), normal hexagonal phase (H_1) consisting of hexagonally packed cylindrical micelles, the viscous isotropic phase (V_1) consisting of a cubic arrangement of non-spherical aggregates, a lamellar phase (L_α) consisting of planar bilayer surfactant sheets separated by water films and an isotropic liquid phase. Each single phase region is separated by a two-phase region containing a mixture of both adjacent phases. At the experimental temperature of 25 °C, pure $C_{12}E_6$ is a liquid.

Fig. 6 shows a comparison of calculated and measured evaporation rates for a total of seven runs starting at different initial compositions. The rates are plotted as the product Eh (which normalises out differences in the stagnant layer thickness h) vs. water mole fraction. For the water-rich compositions ($X_{water} > 0.85$) measured rates are only slightly slower than predicted, indicating that the vapour pressures at the mixture surface are only slightly lower than those predicted from the overall composition, i.e. the mixtures have not developed large concentration gradients. No large rate changes are observed as the phase boundaries from the L_1 to H_1, V_1 and L_α phases are crossed. At the end of the first run (at which point the average value of X_{water} has dropped to approximately 0.9 after evaporating for approximately 11 days) the evaporation rate is approximately 20% lower than the start of run 2 (with an initial, homogeneous X_{water} of approximately 0.9). The 20% rate reduction at the end of run 1 corresponds to a surface composition with X_{water} of 0.65 or so, significantly lower than the overall, average X_{water} of 0.9. The development of this concentration gradient in run 1 (over 11 days) is a very slow process. For run 2, a sharp drop in rate is observed at X_{water} around 0.83 to give a rate of only approximately 10% of that expected for the mixture in the absence of concentration gradients. For run 3, starting at $X_{water} = 0.82$ or so, the initial rate is low indicating that a large concentration gradient has developed within the time between sample preparation and the start of the measurement (approximately 15 minutes). Runs 4–6 (Fig. 6b) show that large concentration gradients resulting in approximately 10 fold rate reductions are again formed relatively rapidly for X_{water} from 0.67 to 0.47. For low water contents (X_{water} from 0.25 to 0.1, Fig. 6c) the measured rates approach the calculated values more closely. This is consistent with the fact that pure $C_{12}E_6$ is a liquid at 25 °C, i.e. the concentration gradient development of the liquid is reduced in this regime.

Overall, structuring of the mixtures resulting in concentration gradient development and evaporation rate reduction is strongest for mid-range mole fractions (X_{water} from approximately 0.83 to 0.4, corresponding to water mass fractions
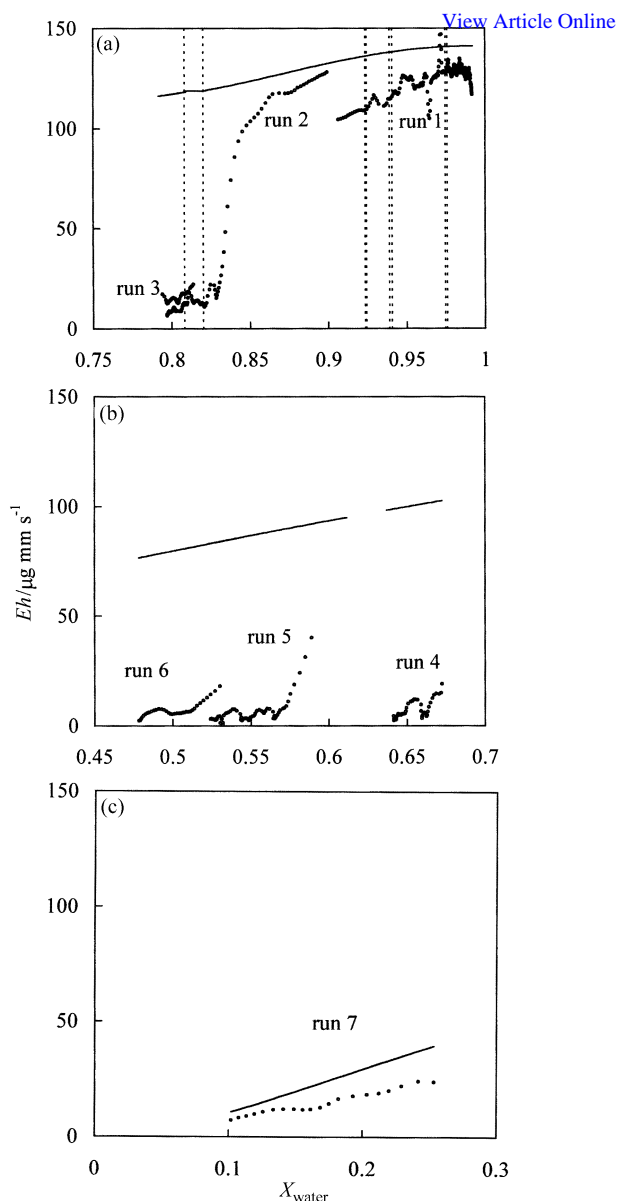

Fig. 6 Comparison of measured (circles) and calculated (solid lines) variation of Eh for mixtures of water and $C_{12}E_6$. A total of seven runs with different initial compositions are shown in plots (a)–(c). The vertical dashed lines show the phase boundaries listed in Table 2.

from 0.16 to 0.03) and shows no correlation with mesophase boundaries in this system. Evaporation rate reduction is expected when the time required for the relaxation of the concentration gradients in the liquid phase is slow relative to the time required for vapour diffusion across the stagnant gas layer. Detailed modelling of the rate reductions therefore requires estimation of mass transfer by diffusion and convection within the microstructured (and commonly multi-phase) liquid mixtures and has not been attempted here. The experimental method and analysis described here allows the estimation of the surface concentration of the evaporating species during the course of evaporation (by comparison of the measured rate with the overall composition predicted to give the same rate) but does not yield the full composition profile within the liquid.

There is (to our knowledge) no literature data for liquid mixture evaporation rates measured through a well defined stagnant gas layer which can be quantitatively compared with the present data. Probably the most closely related data is that of the group of Friberg who have measured evaporation from a range of complex liquid mixtures, particularly emul-

Table 2 Equilibrium phase boundaries for $C_{12}E_6$ plus water mixtures at 25 °C

X_{water} range	Phases present
1–0.9758	Isotropic micellar L_1
0.9758–0.9746	Isotropic micellar L_1 + normal hexagonal H_1
0.9746–0.9406	Normal hexagonal H_1
0.9406–0.9389	Normal hexagonal H_1 + viscous isotropic V_1
0.9389–0.9243	Viscous isotropic V_1
0.9243–0.9235	V_1 + lamellar L_α
0.9235–0.8201	Lamellar L_α
0.8201–0.8082	Lamellar L_α + isotropic liquid
0.8082–0	Isotropic liquid

sions, contained in watch glasses under constant air flow but unspecified stagnant layer thickness (see, for example, ref. 11–13). In one such study,[13] a sharp decrease in evaporation rate was noted when the compositions of emulsions prepared from two isotropic phases reached a three phase region including a lamellar liquid crystalline phase. The strong rate reduction was found to be associated with the formation of a film of lamellar phase on the emulsion surface. In this situation the surface composition (and hence the evaporation rate) is determined by that of the lamellar film and is expected to be very different from the overall, average composition of the three phase mixture. When evaporation was continued until the single phase lamellar phase region was entered, no large reduction in evaporation rate was observed. This latter observation is similar to the behaviour of the $C_{12}E_6$/water system for which we see no large changes in evaporation rates at the overall compositions corresponding to the various mesophase boundaries.

Conclusions

(1) The evaporation rates of pentane and hexane from mixtures with squalane are limited by vapour diffusion rates across the stagnant gas layer. Mixing (probably by convection) within the liquid phases is rapid relative to this process.

(2) Evaporation rates of hexane gelled with silica particles are similar to those of the pure, un-gelled liquid because the hexane vapour pressure is unaffected by the addition of the silica particles.

(3) Water evaporation rates from mixtures with the nonionic surfactant $C_{12}E_6$ are reduced approximately 10 fold owing to the development of concentration gradients within the mixtures. This effect is strongest for water mole fractions

from 0.4 to 0.83 and shows no correlation with the mesophase boundaries.

Acknowledgements

References

1   K. J. Beverley, J. H. Clint and P. D. I. Fletcher, *Phys. Chem. Chem. Phys.*, 1999, **1**, 149.
2   K. J. Beverley, J. H. Clint, P. D. I. Fletcher and S. Thubron, *Phys. Chem. Chem. Phys.*, 1999, **1**, 909.
3   J. H. Clint, P. D. I. Fletcher and I. T. Todorov, *Phys. Chem. Chem. Phys.*, 1999, **1**, 5005.
4   A. J. Ashworth and D. H. Everett, *Trans. Faraday Soc.*, 1960, **56**, 1609.
5   *Selected Values of Properties of Hydrocarbons and related Compounds*, Thermodynamics Research Center, AP144, Texas A&M University, 1978.
6   B. Simon, in *Dynamics of Multiphase Flows across Interfaces*, ed. A. Steinchen, Springer, Berlin, 1996, p. 90.
7   J. S. Clunie, J. F. Goodman and P. C. Symons, *Trans. Faraday Soc.*, 1969, **65**, 287.
8   See, for example, F. MacRitchie, *Chemistry at Interfaces*, Academic Press, San Diego, 1990, p. 175–178 and references therein.
9   N. M. van Os, J. R. Haak and L. A. M. Rupert, *Physico-Chemical Properties of Selected Anionic, Cationic and Nonionic Surfactants*, Elsevier, Amsterdam, 1993.
10 D. J. Mitchell, G. J. T. Tiddy, L. Waring, T. Bostock and M. P. McDonald, *J. Chem. Soc., Faraday Trans. 1*, 1983, **79**, 975.
11 S. E. Friberg and I. Kayali, *J. Pharm. Sci.*, 1989, **78**, 639.
12 S. E. Friberg and B. Langlois, *J. Dispersion Sci. Technol.*, 1992, **13**, 223.
13 B. R. C. Langlois and S. E. Friberg, *J. Soc. Cosmet. Chem.*, 1993, **44**, 23.